RSC Advances

PAPER

View Article Online
View Journal | View Issue

Cite this: *RSC Adv.*, 2021, **11**, 13304

Fluorinated MIL-101 for carbon capture utilisation and storage: uptake and diffusion studies under relevant industrial conditions†

Paola A. Sáenz Cavazos,[a] Mariana L. Díaz-Ramírez,[b] Elwin Hunter-Sellars,[a] Sean R. McIntyre,[a] Enrique Lima,[b] Ilich A. Ibarra*[b] and Daryl R. Williams*[a]

Carbon capture utilisation and storage (CCUS) using solid sorbents such as zeolites, activated carbon and Metal–Organic Frameworks (MOFs) could facilitate the reduction of anthropogenic CO_2 concentration. Developing efficient and stable adsorbents for CO_2 capture as well as understanding their transport diffusion limitations for CO_2 utilisation plays a crucial role in CCUS technology development. However, experimental data available on CO_2 capture and diffusion under relevant industrial conditions is very limited, particularly for MOFs. In this study we explore the use of a gravimetric Dynamic Vapour Sorption (DVS) instrument to measure low concentration CO_2 uptake and adsorption kinetics on a novel partially fluorinated MIL-101(Cr) saturated with different water vapour concentrations, at ambient pressure and temperature. Results show that up to water $P/P_0 = 0.15$ the total CO_2 uptake of the modified material improves and that the introduction of small amounts of water enhances the diffusion of CO_2. MIL-101(Cr)-4F(1%) proved to be a stable material under moist conditions compared to other industrial MOFs, allowing facile regeneration under relevant industrial conditions.

Received 10th February 2021
Accepted 31st March 2021

DOI: 10.1039/d1ra01118a

rsc.li/rsc-advances

Introduction

It is well known that clean energy sources and carbon capture utilisation and storage (CCUS) are vital for climate change mitigation and limiting global warming. However, due to a variety of technical, economic and commercial challenges CCUS has not been fully deployed to the required scale.[1,2] According to the Global Carbon Capture and Storage (CCS) Institute there are 51 large-scale CCS facilities around the world, of which, only 19 are fully operating and an estimated 2000 more are needed to achieve global climate targets.[2]

Large-scale projects that utilize CO_2 capture with solid state adsorbents are few compared to the widely used liquid absorption technologies.[1] One of the main reasons for this difference is the enormous variety of available potential adsorbent materials, which makes the screening process for CCS sorbents tremendously challenging. Particularly in the case of Metal–Organic Frameworks (MOFs) which have an inherent adsorption tunability due to their unique chemical structure. MOFs ability to incorporate open metal sites (OMSs), Lewis basic sites (LBSs), covalently bound polar functional groups, framework flexibility, and hydrophobicity offers thousands of 'tailor design' possibilities to enhance adsorption capacity, selectivity, and stability.[1,3]

While high-throughput simulation and modelling techniques have been shown to greatly accelerate the pace of identifying promising candidates for CO_2 capture, their evaluation criteria usually concerns a single adsorption or material property at a time.[4–7] For instance, Wilmer *et al.* established correlations between CO_2/N_2 separation ability based solely on MOFs structural and chemical characteristics without considering the other additional components present in industrial flue gases, like water vapour, oxygen and acidic gases (*i.e.* H_2S, NO_x, SO_x).[7] Going one step further, Li *et al.* identified potential MOFs for Post-combustion Carbon Capture (PCC) in the presence of high relative humidity (RH) 80% based on their CO_2/H_2O selectivity.[5] Though understanding MOFs performance at high RH's is important, the amount of water usually present in the flue gas is around 4–18% RH.[8–10] In addition, and very interestingly, various studies have confirmed that the presence of low amounts of water can sometimes enhance the CO_2 uptake of several materials.[11–15] From a cost perspective, Huck *et al.* proposed a new approach for material evaluation based on parasitic energy which is a metric that predicts the total energy penalty imposed on a CCS power plant using porous adsorbents based on a thermodynamic analysis.[4] What all these approaches fail to consider is several relevant industrial conditions

[a]*Surfaces and Particle Engineering Laboratory (SPEL), Department of Chemical Engineering, Imperial College London, South Kensington Campus, London SW7 2AZ, UK. E-mail: d.r.williams@imperial.ac.uk*

[b]*Laboratorio de Fisicoquímica y Reactividad de Superficies (LaFReS), Instituto de Investigaciones en Materiales, Universidad Nacional Autónoma de México, Circuito Exterior s/n, CU, Coyoacán, 04510 Ciudad de México, Mexico. E-mail: argel@unam.mx*

† Electronic supplementary information (ESI) available: Figures and additional characterization. See DOI: 10.1039/d1ra01118a

simultaneously, due mainly to the lack of experimental data needed to develop such complex models.

Additionally, some MOFs can capture and convert CO_2 at the same time. MOF's high surface area and porous structure provide favourable catalytic efficiencies and high reaction yields, with some of these bifunctional materials allowing a direct transition from CCS to CCUS.[8,16] Understanding transport diffusion limitations in MOFs could positively influence the catalyst effectiveness and facilitate the design of adsorption processes.[17] Nevertheless, this information requirement adds another level of complexity to the adsorbent screening process because the data available on mass-transfer resistance and diffusion limitations for MOFs is still scarce.[1,3] Fast and accurate characterisation techniques that provide crucial experimental data on solid sorbents, when linked together with molecular simulation and process-scale modelling are particularly desirable to move on to the next technology readiness level.[1,3,16]

In this study we investigate the use of a gravimetric Dynamic Vapour Sorption (DVS) instrument as a rapid characterisation technique for novel adsorbent materials that permits several relevant industrial conditions to be investigated, allowing a range of equilibrium and kinetics descriptors of the adsorption process to be determined. In order to highlight the tunability and bifunctionality of MOFs we chose MIL-101(Cr)-4F(1%) as our material for this case study. This material is the result of the successful partial fluorination of MIL-101(Cr); which we achieved recently.[18] MIL-101(Cr)-4F(1%) showed an increased hydrophobicity and a higher selectivity towards CO_2 in anhydrous conditions when compared to its pristine form MIL-101(Cr).[18] Furthermore, MIL-101(Cr) based composites have shown outstanding catalytic activity (96.5% yield) in the conversion of terminal alkynes into propiolic acids with CO_2, as well as in several other carbon conversion reactions.[3,19,20]

The DVS instrument was used to measure and analyse adsorption and co-adsorption of low concentration CO_2 and H_2O on the enhanced material and its pristine form at ambient pressure and temperature (298 K and 1 bar), attempting to replicate real industrial conditions. To further understand the CO_2 diffusion limitations in the presence of water vapour of these materials, we used the gravimetric kinetic data collected and determined the CO_2 diffusion coefficient as a function of water vapour concentration. To the best of our knowledge, this study is the first time CO_2 experiments under the presence of water vapour are reported on this material. The data obtained in this study on MIL-101(Cr)-4F(1%) and MIL-101(Cr) provides a broader understanding of novel materials capabilities for carbon capture and conversion under pertinent industrial conditions.

Experimental

Materials

MIL-101(Cr) and MIL-101(Cr)-4F(1%) were synthesised as described in previous literature.[18] Samples were activated at 453 K under vacuum (10^{-3} bar) for 2 h before every experiment to ensure any contaminants or excess moisture were removed. Commercial MOF samples of HKUST-1 and MIL-53(Al) were purchased from BASF and activated using the same process mentioned above.

Sorption measurements

All sorption measurements were carried out gravimetrically using a DVS Resolution (Surface Measurement Systems, UK) using an electronic microbalance with a resolution of ± 0.01 μg and a symmetric measurement configuration. Meaning that both, the sample pan, and the reference pan are exposed to the same gas at the same temperature and ambient pressure, thus minimising buoyancy effects. The balance itself is fitted inside a stainless-steel housing unit which is mounted above the gas/vapor adsorption manifold. The entire balance manifold system is located inside a temperature enclosure that maintains a temperature uniformity of <0.1 K. A series of mass flow controls allows gas mixtures containing air, CO_2 and H_2O to be prepared which flow over the adsorbent sample. The relative humidity and CO_2 concentration within the gas stream are measured in real time with capacitance and speed of sound sensors respectively.

The equipment was leak checked before each experiment by measuring the system output gas flowrate with an independent mass flow meter (Agilent Technologies, USA) and comparing it to the system input flowrate, ensuring both values were always the same. After sample activation, 10–30 mg of sample was placed inside the sample pan for measuring water and CO_2 isotherms at 298 K and 1 bar. Sufficient time was allowed for the samples to reach mass equilibrium at each of the user selected gas phase concentrations, until no significant mass change was detected (<0.00075% min^{-1} dm/dt). The equipment recorded the change in mass *versus* time using the DVS software. A total flow rate of 200 cm^3 min^{-1} of dry air was used as carrier gas. We also performed single component experiments using pure N_2 as a carrier gas and no significant difference in water or CO_2 uptake was observed. In order to better simulate "real world" conditions dry air containing ~78% N_2 and ~21% O_2 was used throughout all experiments.

Co-adsorption measurements

Co-adsorption measurements were carried out using the dual-solvent mode of the DVS Resolution. Following activation, samples were exposed to a selected range of partial pressure of water vapour to simulate flue gas composition ($P/P_{0,water} = 0$, 0.05, 0.1, 0.15 and 0.2), and while this pressure was held constant, a step increase in CO_2 concentration to 0.05 bar was introduced, followed by desorption of CO_2 and finally desorption of water vapour.

Considering that we were also interested in the kinetic CO_2 sorption profiles from the co-adsorption measurements to extract CO_2 diffusion coefficients. Smaller sample masses (5–20 mg) widely dispersed in the sample pan were used to avoid bed resistances and heat transfer limitations.[21] All steps were carried out at constant temperature and total pressure (298 K and 1 bar). Enough time was allowed for the samples to reach equilibrium with the gas phase until no significant mass change

was detected (0.00075% min^{-1} dm/dt). Dry air with a total flow rate of 400 cm^3 min^{-1} was used as carrier gas. This methodology has been previously used in other studies to measure multi-component sorption.[22,23]

Particle size

A sieve analysis using test sieves of different aperture 250, 180 and 90 μm (Endecotts Ltd, UK) and an automatic sieve shaker from the same manufacturer allowed to determine the average particle size of the materials studied. The ASTM standard test method for particle size distribution of catalytic materials by sieving was applied.[24]

Results and discussion

Water isotherms

The shape of the water isotherm of the functionalised material at 295 K and 1 bar (see Fig. 1) corresponds to that of a mesoporous solid with a Type V isotherm, where multilayer adsorption is observed at low partial pressures 0 to 0.2 P/P_0, followed by a clear hysteresis loop between 0.2 and 0.6 P/P_0 that can be associated with capillary condensation taking place in the mesopores. The maximum water uptake for MIL-101(Cr)-4F(1%) was 49.1 mmol g^{-1}, which is lower than that reported for the pristine material under the same conditions (55.5 mmol g^{-1}).[25] This data supports an overall augmented hydrophobicity that can be attributed to the incorporation of fluorine atoms in this material.[18]

CO_2 isotherms

CO_2 adsorption isotherms of MIL-101(Cr) and MIL-101(Cr)-4F(1%) were obtained at ambient pressure and temperature (298 K and 1 bar). Both isotherms present a linear behaviour (see Fig. 2). The CO_2 uptake of the two materials is very similar up to 0.6 bar, whereas at higher partial pressures the pristine material shows a slightly increased CO_2 uptake. This can be attributed to the lower pore volume of MIL-101(Cr)-4F(1%)

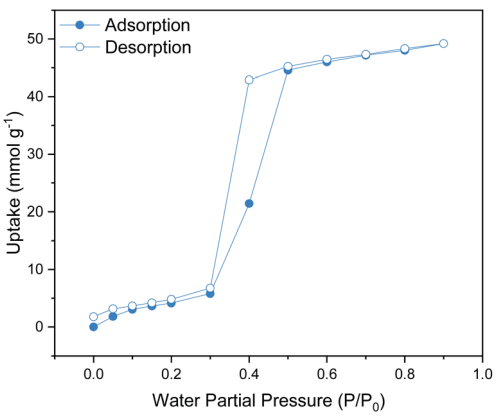

Fig. 1 Water (H_2O) adsorption–desorption isotherms at 298 K and 1 bar of MIL-101(Cr)-4F(1%) from $P/P_0 = 0$ to 0.9. Solid circles represent adsorption and open circles represent desorption.

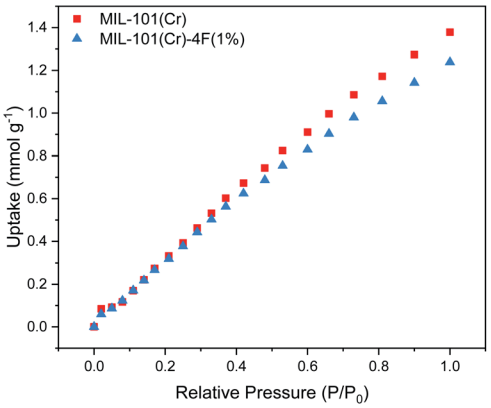

Fig. 2 Carbon dioxide (CO_2) adsorption isotherms at 298 K and 1 bar of MIL-101(Cr) and MIL-101(Cr)-4F(1%) relative CO_2 partial pressures range from $P/P_0 = 0$ to 1.0.

compared to MIL-101(Cr), 1.19 cm^3 g^{-1} and 1.32 cm^3 g^{-1} respectively.[18]

Given that the pressure region we are interested in for PCC applications is between 0 and 0.2 bar, we can say that both materials have comparable CO_2 uptakes within this region. However, MIL-101(Cr)-4F(1%) has the advantage of being more hydrophobic, making it less vulnerable when exposed to moist environments and a better candidate than MIL-101(Cr) under real industrial capture conditions.[26,27]

Co-adsorption of water and CO_2

Encouraged by the results from a previous work,[18] where we showed that CO_2 moves easier through MIL-101(Cr) than through MIL-101(Cr)-4F(1%) due to a less acidic nature of Cr(III) sites on the pristine material, and considering that the CO_2 level present in flue gases is regularly between 4–14% in volume,[28] we decided to explore the effects of low concentration CO_2 sorption and diffusion under humid conditions on both materials. We hypothesised that the introduction of small amounts of water in the framework of MIL-101(Cr) and MIL-101(Cr)-4F(1%) would promote the transport of CO_2 through the materials. This is because water molecules would occupy the coordinatively unsaturated sites (CUS) resulting from the activation of the material. In small amounts, the water molecules would be well-ordered inside the MOF cavities providing a smoother path for incoming CO_2 molecules and would also lower the strength of the interactions of the framework with the CO_2.

Five different RH concentrations were studied 0, 10, 15 and 20%, which correspond to water partial pressures of 0, 0.05, 0.10, 0.15 and 0.20 P/P_0 respectively. For all RH's the CO_2 concentration was kept constant at 5%, which corresponds to a CO_2 pressure of 0.05 bar in ambient conditions. The data obtained from a typical co-adsorption experiment consists of four steps, two for adsorption and two for desorption (see Fig. 3). CO_2 uptake was calculated by subtracting the mass at the end the second step from the mass at the end of the first step. The results from the co-adsorption experiments are presented in Fig. 4. For dry materials, *i.e.* $P/P_0 = 0$, the partially fluorinated

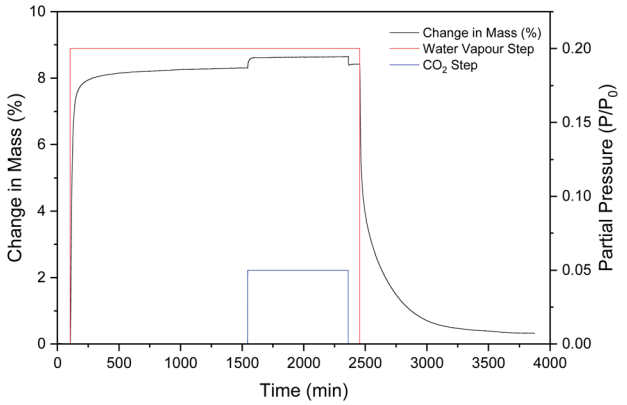

Fig. 3 Adsorption and desorption mass change of MIL-101(Cr) exposed to a step change of water partial pressure of 0.2 P/P_0, followed by a CO_2 partial pressure step change of 0.05 bar at 298 K and 1 bar.

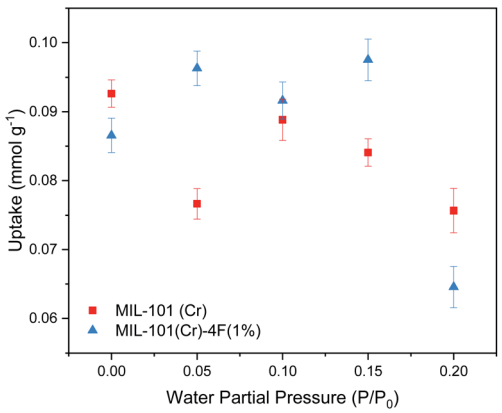

Fig. 4 Carbon dioxide (CO_2) adsorption capacities of MIL-101(Cr) and MIL-101(Cr)-4F(1%) of CO_2 P/P_0 = 0.05 at different water partial pressures (0, 0.05, 0.1, 0.15 and 0.2 P/P_0) at 298 K and 1 bar.

material has a very slight lower CO_2 uptake than its pristine form (0.086 *vs.* 0.092 mmol g^{-1}, respectively) which agrees with our previous findings from the single component CO_2 isotherms. However, the materials behave very differently when water vapour is present. For MIL-101(Cr) the presence of water is detrimental for its performance, with CO_2 capacity decreasing at higher water partial pressures, up to the highest value studied (P/P_0 = 0.2), where its CO_2 uptake decreases by around 18% compared to the dry material.

MIL-101(Cr) shows no direct proportionality between the CO_2 adsorption capacity and the quantity of water present on the sample, which agrees with previous findings.[29] On the other hand, MIL-101(Cr)-4F(1%) shows a CO_2 uptake enhancement at low and moderate water loadings, reaching a maximum uptake of 0.097 mmol g^{-1} at P/P_0 = 0.15. Nevertheless, at P/P_0 = 0.2 bar the fluorinated material shows a 22% lower CO_2 uptake compared to the dry material. This behaviour can be attributed to the loss of terminal water molecules in the Cr–O cluster during the activation of the material, complete loss of these water molecules means that some favoured CO_2 adsorption sites may be lost as well. However, with increasing RH values, some of these adsorption sites are recovered and therefore, the uptake improves. There is a value of RH where the presence of H_2O molecules has no longer a positive effect, and rather, these molecules compete for adsorption sites with CO_2. This phenomenon has been previously observed in other MOFs with CUS, such as Cu-BTC[30] and UiO-66.[31] It is important to mention that while the CO_2 uptake of the materials studied is not exceptional under real industrial conditions, they are both very stable when exposed to moist environments, compared to other commercial materials such as HKUST-1 or MIL-53(Al). Specifically, under the same conditions, where their CO_2 uptake at water P/P_0 = 0.2 decreases by 99% and 80% respectively compared to their dry form (see Fig. S2 ESI†). Further CO_2 enhancement on the fluorinated material could be achieved by the incorporation of amine groups such as alkylamines, polyamines or multiunit amines *via* wet impregnation methods. This has shown to improve MOFs CO_2 adsorption capacity and regeneration stability in dilute CO_2 concentrations due to the high amine–CO_2 reaction equilibrium constants, but is not in the scope of this study.[32,33]

Following adsorption, we studied the desorption of CO_2 at different RHs. Desorption under these conditions is extremely relevant to the adsorbent regeneration step during temperature and pressure swing adsorption processes.[34] Decreasing the energy requirements for this stage is crucial for the cost reduction and feasibility of CCS technologies.[1,34] We observed that both materials, when dry, they were able to desorb ~50% of the CO_2. Fig. 5 shows the results once water is introduced. Since we are using a gravimetric technique, we measured the mass at the end of the last step for every experiment and compared it to the water adsorption isotherm. The results indicate that there is some water being re-absorbed or that some CO_2 remains within the framework. If the latter is considered, we can say that at P/P_0 = 0.05 the percent of CO_2 desorbed increased to 90.32% and 71.80% for MIL-101(Cr) and MIL-101(Cr)-4F(1%) respectively. This could be because the water is promoting the transport of

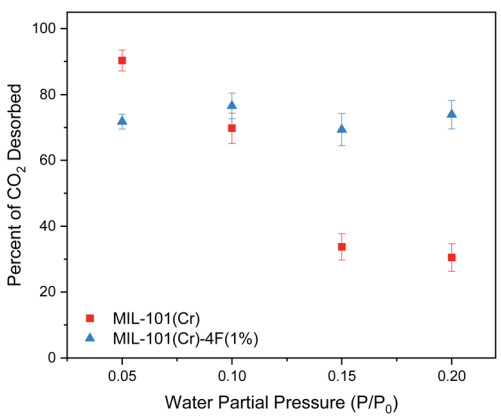

Fig. 5 Percent of carbon dioxide (CO_2) desorbed on MIL-101(Cr) and MIL-101(Cr)-4F(1%) with different water partial pressures (0, 0.05, 0.1, 0.15 and 0.2 P/P_0) at 298 K and 1 bar.

CO_2 in the desorption step as well. As mentioned before the less acidic nature of Cr(III) allows for easier movement of the CO_2 molecules through MIL-101(Cr) and thus the difference between the pristine form and the fluorinated one. Fig. 5 clearly indicates a stable amount of CO_2 desorbed in MIL-101(Cr)-4F(1%) throughout all the RH studied, whereas for the pristine material, a decreasing trend can be observed. This could be related to the more hydrophobic nature of the material incorporated with fluorine atoms and could potentially translate in a reduction of the energy needed to desorb the remaining CO_2. Thus, giving rise to MIL-101(Cr)-4F(1%) as a promising candidate for PCC.

Additionally, ensuring the material is stable during various adsorption–desorption cycles and in the presence of other contaminants such as acidic gases could further help decrease costs.[1] Remarkably, MIL-101(Cr)-4F(1%) has shown high SO_2 capture under humid conditions and an outstanding cycling performance up to 50 cycles with facile regeneration.[35] For industrial scale applications it is also important to consider the competition for adsorption sites with other acidic gases present in the flue gas, however this is not in the scope of the present study.

Determination of diffusion coefficients

Adsorption efficiency is greatly influenced by both equilibrium and kinetics.[36] Therefore, determining parameters such as diffusivity is of great interest.

Moreover, understanding diffusion limitations of MOFs is important for future catalytic applications in CCUS. In this study we used the dynamic gravimetric uptake curves from the co-adsorption experiments to determine adsorption kinetics and extract the CO_2 diffusion coefficients of MIL-101(Cr) and MIL-101(Cr)-4F(1%) at a range of different water vapour concentrations.

The gravimetric instrument settings during the adsorption–desorption experiments were selected in order to minimize heat transfer and external mass transfer resistances.[21] Firstly, we verified that the uptake experiments were slow enough so as to not mistake mass transfer with instrument response time. Fig. 6 shows the gravimetric measurement of 0.05 bar CO_2 in MIL-101(Cr)-4F(1%) for different sample masses. The curves have a timescale in the order of 250 minutes and according to the manufacturer the system response time is <1 minute.[37] Therefore, mass transfer kinetics can be measured accurately by assuming drag and buoyancy effects reach steady state almost immediately.[21] Then, extra-crystalline diffusion and heat transfer control can also be avoided by changing the sample mass and obtaining consistent results (see Fig. 6).[21,38] Finally, small amounts of sample were used to avoid bed resistances and heat transfer limitations.[21]

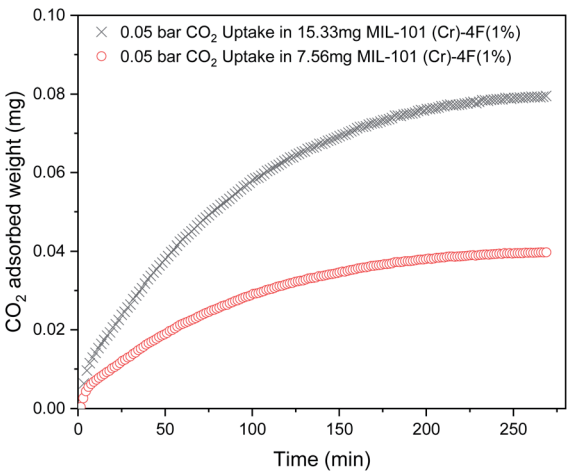

Fig. 6 Carbon dioxide (CO_2) gravimetric experiment uptakes for 15.33 mg and 7.56 mg MIL-101(Cr)-4F(1%) at 298 K and 0.05 bar.

We assumed spherical particles for both materials and determined the CO_2 diffusion coefficients in the presence of different water vapour concentrations using the following model (see eqn (1)).[21,39] This model is derived from Fick's second law of diffusion and it is a good approximation for slow diffusing systems.

$$\frac{M_t}{M_\infty} = 1 - \frac{6}{\pi^2}\sum_{n=1}^{\infty}\frac{1}{n^2}\exp\left(-\frac{n^2\pi^2 Dt}{r_p^2}\right) \quad (1)$$

where, M_t/M_∞ is the ratio between the mass at a given time t and the mass at time equals infinity or equilibrium mass, and r_p is the particle radius. When $M_t/M_\infty < 0.2$, eqn (1) can be simplified to eqn (2).[39] Kinetic data (Fig. S3 ESI†), was normalized and plotted against the square root of time (Fig. S4 ESI†) along with a linear fit up to 0.2. By substituting the value of the slope from the linear fit into eqn (2) and solving for D, we can obtain the CO_2 diffusion coefficient.

$$\frac{M_t}{M_\infty} = \frac{6}{r_p}\sqrt{\frac{Dt}{\pi}} \quad (2)$$

In order to determine the particle radius, the particle size distribution of MIL-101(Cr) and MIL-101(Cr)-4F(1%) was estimated using test sieves. Tables S1 and S2 ESI† show the results for each material. The average particle size can be found by plotting the cumulative percentage data against the sieve aperture and determining the size corresponding to 50%. The average particle radius of MIL-101(Cr) and MIL-101(Cr)-4F(1%) was 104 μm and 96 μm respectively. Table 1 shows the diffusion coefficients of MIL-101(Cr) and MIL-101(Cr)-4F(1%) at different water vapour loadings. The values obtained in this study fall in the range of experimental diffusion coefficients found for pure CO_2 in MOFs or porous solids.[40,41] The diffusion coefficient of both materials studied in dry conditions, is in the order of 8.6×10^{-10} and 5.0×10^{-10} $cm^2\ s^{-1}$ for MIL-101(Cr) and MIL-101(Cr)-4F(1%), respectively. This means CO_2 is able to move faster through the pristine material, conceding with what was reported in our previous study.[18]

A small increase in water *i.e.*, at $P/P_0 = 0.05$ results in an easier transport of CO_2, because water molecules adsorb on the most attractive sites for adsorption (*i.e.*, open metal sites) providing a more homogeneous surface and consequently allowing CO_2 molecules to move more freely. This phenomena

Table 1 Carbon dioxide (CO_2) diffusion coefficients of MIL-101(Cr) and MIL-101(Cr)-4F(1%) at different water partial pressures

Water partial pressure P/P_0	MIL-101(Cr)		MIL-101(Cr)-4F(1%)	
	D/r_p^2	D ($cm^2\ s^{-1}$)	D/r_p^2	D ($cm^2\ s^{-1}$)
0	8.0×10^{-6}	$8.6 \times 10^{-10} \pm 2 \times 10^{-11}$	5.4×10^{-6}	$5.0 \times 10^{-10} \pm 1 \times 10^{-11}$
0.05	2.7×10^{-4}	$2.9 \times 10^{-8} \pm 1 \times 10^{-11}$	1.5×10^{-4}	$1.3 \times 10^{-8} \pm 2 \times 10^{-11}$
0.1	2.6×10^{-4}	$2.8 \times 10^{-8} \pm 1 \times 10^{-11}$	1.5×10^{-4}	$1.3 \times 10^{-8} \pm 2 \times 10^{-11}$
0.15	2.7×10^{-4}	$2.8 \times 10^{-8} \pm 1 \times 10^{-11}$	1.7×10^{-4}	$1.5 \times 10^{-8} \pm 1 \times 10^{-11}$
0.20	2.3×10^{-4}	$2.4 \times 10^{-8} \pm 1 \times 10^{-11}$	5.9×10^{-5}	$5.3 \times 10^{-9} \pm 1 \times 10^{-11}$

is clearly observed with the diffusion coefficient values increasing in two orders of magnitude, 2.9×10^{-8} for MIL-101(Cr) and 1.3×10^{-8}, for MIL-101(Cr)-4F(1%). For P/P_0 between 0.05 and 0.15 the diffusion coefficients of the two materials remain almost unchanged, while for high water partial pressures *i.e.*, at $P/P_0 = 0.2$ the diffusion coefficient drops. Very interestingly, the decrease observed is more prominent on the fluorinated material compared to the pristine form.

Where the diffusion coefficient drops from 1.5×10^{-8} to 5.3×10^{-9}. This could be related to the dramatic loss that we also observe with the CO_2 uptake in MIL-101(Cr)-4F(1%) at the highest water partial pressure studied ($P/P_0 = 0.2$) (see Fig. 4). However, the lowest diffusion coefficient for MIL-101(Cr)-4F(1%) does not coincide with the partial pressure that has the highest CO_2 uptake.

This indicates that in order promote the interaction between the CO_2 molecules and the porous material an optimum rate of transport must be achieved. This means, not too slow that the trapped molecules can block and thus impeding other molecules to pass, but not so fast that the molecules are not able to interact with the framework. A trade-off between uptake and kinetics should ultimately be considered depending on the specific process application.

Conclusions

Understanding the effects of different flue gas composition and conditions in the adsorption and kinetics of solid sorbents for CO_2 capture is of great importance for CCUS technology to advance.

In this study a single experimental technique (Dynamic Vapour Sorption, DVS) was used to determine CO_2 uptake and adsorption kinetics of low concentration CO_2 with different water vapour concentrations (0.0, 0.05, 0.10, 0.15 and 0.20) on MIL-101(Cr)-4F(1%) and its pristine form MIL-101(Cr). All experiments were carried out at ambient pressure and temperature to resemble economically feasible industrial conditions. Our results show that at low and moderate water loadings the total CO_2 uptake capacity of MIL-101(Cr)-4F(1%) improved, with the best uptake (0.097 CO_2 mmol g^{-1}) at $P/P_0 = 0.15$. However, higher partial pressures seem to inhibit CO_2 uptake. As for the pristine material, the highest water loading decreases it's overall CO_2 capacity by 18% compared to its dry form. Both materials present a stable behaviour in moist environments when compared to other commercial adsorbents with higher CO_2 capacity (HKUST-1 and MIL-53(Al)) under the same conditions. Desorption results of CO_2 with different water loadings at ambient pressure and temperature suggest that the fluorinated material would have a minimum energy penalty during the regeneration step.

CO_2 diffusion coefficients at different water partial pressures were extracted from the mass uptake curves of the co-adsorption experiments. For both materials, CO_2 diffusion occurs faster when water is introduced; this is because water is responsible for providing a more homogeneous surface and permits an easier movement for CO_2. For water concentrations from $P/P_0 = 0.05$ to 0.15 the CO_2 diffusion coefficients of both materials remain stable, however, at the maximum water partial pressure studied $P/P_0 = 0.2$ a drop in the diffusion coefficient in the fluorinated material can be observed, coinciding with a drop in CO_2 uptake. This data suggests that certain water vapour concentrations of up to 0.15 P/P_0 can promote CO_2 diffusion which coincidentally corresponds to the water concentrations of most industrial importance for CCS. Above these conditions, a compromise between uptake and transport kinetics should be considered.

Conflicts of interest

There are no conflicts to declare.

Acknowledgements

The authors would like to thank PAPIIT UNAM (IN202820), México for financial support. M. L. D.-R. thanks CONACyT, México for the PhD grant number 276862. U. Winnberg and G. Ibarra-Winnberg for scientific input. P. A. S.-C would like to thank CONACyT-SENER for the PhD grant in Energy and Sustainability.

References

1 M. Bui, C. S. Adjiman, A. Bardow, E. J. Anthony, A. Boston, S. Brown, P. S. Fennell, S. Fuss, A. Galindo, L. A. Hackett, J. P. Hallett, H. J. Herzog, G. Jackson, J. Kemper, S. Krevor, G. C. Maitland, M. Matuszewski, I. S. Metcalfe, C. Petit, G. Puxty, J. Reimer, D. M. Reiner, E. S. Rubin, S. A. Scott, N. Shah, B. Smit, J. P. M. Trusler, P. Webley, J. Wilcox and N. Mac Dowell, *Energy Environ. Sci.*, 2018, **11**, 1062–1176.

2 G. C. Institute, *Global Status of CCS: Brief for Policymakers*, 2020, https://www.globalccsinstitute.com/resources/publications-reports-research/.
3 M. Ding, R. W. Flaig, H.-L. Jiang and O. M. Yaghi, *Chem. Soc. Rev.*, 2019, **48**, 2783–2828.
4 J. M. Huck, L.-C. Lin, A. H. Berger, M. N. Shahrak, R. L. Martin, A. S. Bhown, M. Haranczyk, K. Reuter and B. Smit, *Energy Environ. Sci.*, 2014, **7**, 4132–4146.
5 S. Li, Y. G. Chung and R. Q. Snurr, *Langmuir*, 2016, **32**, 10368–10376.
6 M. Tong, Y. Lan, Q. Yang and C. Zhong, *Green Energy Environ.*, 2018, **3**, 107–119.
7 C. E. Wilmer, O. K. Farha, Y.-S. Bae, J. T. Hupp and R. Q. Snurr, *Energy Environ. Sci.*, 2012, **5**, 9849–9856.
8 L. Liang, C. Liu, F. Jiang, Q. Chen, L. Zhang, H. Xue, H.-L. Jiang, J. Qian, D. Yuan and M. Hong, *Nat. Commun.*, 2017, **8**, 1233.
9 C. Song, W. Pan, S. T. Srimat, J. Zheng, Y. Li, Y.-H. Wang, B.-Q. Xu and Q.-M. Zhu, in *Studies in Surface Science and Catalysis*, ed. S.-E. Park, J.-S. Chang and K.-W. Lee, Elsevier, 2004, vol 153, pp. 315–322.
10 R. Zevenhoven and P. Kilpinen, *Control of pollutants in flue gases and fuel gases*, Finland, 2001.
11 G. A. Gonzalez-Martinez, T. Jurado-Vazquez, D. Solis-Ibarra, B. Vargas, E. Sanchez-Gonzalez, A. Martinez, R. Vargas, E. Gonzalez-Zamora and I. A. Ibarra, *Dalton Trans.*, 2018, **47**, 9459–9465.
12 V. B. López-Cervantes, E. Sánchez-González, T. Jurado-Vázquez, A. Tejeda-Cruz, E. González-Zamora and I. A. Ibarra, *Polyhedron*, 2018, **155**, 163–169.
13 R. A. Peralta, B. Alcántar-Vázquez, M. Sánchez-Serratos, E. González-Zamora and I. A. Ibarra, *Inorg. Chem. Front.*, 2015, **2**, 898–903.
14 M. Sagastuy-Brena, P. G. M. Mileo, E. Sanchez-Gonzalez, J. E. Reynolds, T. Jurado-Vazquez, J. Balmaseda, E. Gonzalez-Zamora, S. Devautour-Vinot, S. M. Humphrey, G. Maurin and I. A. Ibarra, *Dalton Trans.*, 2018, **47**, 15827–15834.
15 A. Zárate, R. A. Peralta, P. A. Bayliss, R. Howie, M. Sánchez-Serratos, P. Carmona-Monroy, D. Solis-Ibarra, E. González-Zamora and I. A. Ibarra, *RSC Adv.*, 2016, **6**, 9978–9983.
16 J. R. Fernández, S. Garcia and E. S. Sanz-Pérez, *Ind. Eng. Chem. Res.*, 2020, **59**, 6767–6772.
17 H. S. Fogler, *Elements of chemical reaction engineering*, Prentice Hall, Boston, 5th edn, 2016.
18 M. L. Díaz-Ramírez, E. Sánchez-González, J. R. Álvarez, G. A. González-Martínez, S. Horike, K. Kadota, K. Sumida, E. González-Zamora, M.-A. Springuel-Huet, A. Gutiérrez-Alejandre, V. Jancik, S. Furukawa, S. Kitagawa, I. A. Ibarra and E. Lima, *J. Mater. Chem. A*, 2019, **7**, 15101–15112.
19 M. Ding and H.-L. Jiang, *ACS Catal.*, 2018, **8**, 3194–3201.
20 X.-H. Liu, J.-G. Ma, Z. Niu, G.-M. Yang and P. Cheng, *Angew. Chem., Int. Ed*, 2015, **54**, 988–991.
21 J.-Y. Wang, E. Mangano, S. Brandani and D. M. Ruthven, *Adsorption*, 2021, **27**, 295–318.
22 E. Hunter-Sellars, J. J. Tee, I. P. Parkin and D. R. Williams, *Microporous Mesoporous Mater.*, 2020, **298**, 110090.
23 E. Hunter-Sellars, P. A. Saenz-Cavazos, A. R. Houghton, S. R. McIntyre, I. P. Parkin and D. R. Williams, *Adv. Funct. Mater.*, 2020, 2008357.
24 ASTM International, *D4513-11(2017) Standard Test Method for Particle Size Distribution of Catalytic Materials by Sieving*, ASTM International, West Conshohocken, PA, 2017, DOI: 10.1520/D4513-11R17.
25 H. W. B. Teo, A. Chakraborty and S. Kayal, *Appl. Therm. Eng.*, 2017, **120**, 453–462.
26 C. A. Trickett, A. Helal, B. A. Al-Maythalony, Z. H. Yamani, K. E. Cordova and O. M. Yaghi, *Nat. Rev. Mater.*, 2017, **2**, 17045.
27 S. Mukherjee, S. Sharma and S. K. Ghosh, *APL Mater.*, 2019, **7**, 050701.
28 D. Y. C. Leung, G. Caramanna and M. M. Maroto-Valer, *Renewable Sustainable Energy Rev.*, 2014, **39**, 426–443.
29 N. Chanut, S. Bourrelly, B. Kuchta, C. Serre, J. S. Chang, P. A. Wright and P. L. Llewellyn, *ChemSusChem*, 2017, **10**, 1543–1553.
30 A. Ö. Yazaydın, A. I. Benin, S. A. Faheem, P. Jakubczak, J. J. Low, R. R. Willis and R. Q. Snurr, *Chem. Mater.*, 2009, **21**, 1425–1430.
31 A. D. Wiersum, E. Soubeyrand-Lenoir, Q. Yang, B. Moulin, V. Guillerm, M. B. Yahia, S. Bourrelly, A. Vimont, S. Miller, C. Vagner, M. Daturi, G. Clet, C. Serre, G. Maurin and P. L. Llewellyn, *Chem.–Asian J.*, 2011, **6**, 3270–3280.
32 Y. Liu, J. Shi, J. Chen, Q. Ye, H. Pan, Z. Shao and Y. Shi, *Microporous Mesoporous Mater.*, 2010, **134**, 16–21.
33 X. Su, L. Bromberg, V. Martis, F. Simeon, A. Huq and T. A. Hatton, *ACS Appl. Mater. Interfaces*, 2017, **9**, 11299–11306.
34 Y. Lara, L. M. Romeo, P. Lisbona, S. Espatolero and A. I. Escudero, *Energy Technol.*, 2018, **6**, 1649–1659.
35 E. Martínez-Ahumada, M. L. Díaz-Ramírez, H. A. Lara-García, D. R. Williams, V. Martis, V. Jancik, E. Lima and I. A. Ibarra, *J. Mater. Chem. A*, 2020, **8**, 11515–11520.
36 B. Shirani and M. Eic, *Can. J. Chem. Eng.*, 2016, **94**, 2023–2034.
37 S. M. Systems, *DVS Resolution Brochure*, https://www.surfacemeasurementsystems.com/wp-content/uploads/2014/05/DVS-Resolution-brochure-v1.0.pdf, 2020.
38 B. Shirani, X. Han and M. Eic, *Sep. Purif. Technol.*, 2020, **230**, 115831.
39 J. Crank and E. P. J. Crank, *The Mathematics of Diffusion*, Clarendon Press, 1979.
40 Z. Zhao, Z. Li and Y. S. Lin, *Ind. Eng. Chem. Res.*, 2009, **48**, 10015–10020.
41 T. M. Tovar, J. Zhao, W. T. Nunn, H. F. Barton, G. W. Peterson, G. N. Parsons and M. D. LeVan, *J. Am. Chem. Soc.*, 2016, **138**, 11449–11452.